Interplay between Josephson effect and magnetic interactions in double quantum dots

F. S. Bergeret, A. Levy Yeyati, and A. Martín-Rodero

Departamento de Física Teórica de la Materia Condensada C-V, Universidad Autónoma de Madrid, E-28049 Madrid, Spain
(Received 27 February 2006; published 23 October 2006)

We analyze the magnetic and transport properties of a double quantum dot coupled to superconducting leads. In addition to the possible phase transition to a π state, already present in the single dot case, this system exhibits a richer magnetic behavior due to the competition between Kondo and interdot antiferromagnetic coupling. We obtain results for the Josephson current which may help to understand recent experiments on superconductor-metallofullerene dimer junctions. We show that in such a system the Josephson effect can be used to control its magnetic configuration.

　　　　　　PACS number(s): 74.50.+r, 73.21.La, 73.63.−b, 75.20.Hr

Quantum dot (QD) devices provide a unique opportunity to study the interplay between different basic quantum phenomena. Thus, for instance, great advances in the understanding of Kondo physics have been achieved since the observation of the Kondo effect in semiconducting quantum dots.[1] More recently, double quantum dot (DQD) structures have been proposed for studying the competition between the Kondo effect and the interdot antiferromagnetic coupling.[2] An additional interesting ingredient is introduced when these systems are connected to superconducting electrodes.[3] In this case the electron pairing in the leads appears as a competing mechanism to both the Kondo and other type of magnetic interactions that could be present. For a single quantum dot placed between two superconductors this competition can lead to a suppression of the Kondo effect and the appearance of an unscreened magnetic moment, corresponding to a quantum phase transition to the so-called π state with a reversal of the sign of the Josephson current.[4,5] On the experimental side, great progress in the physical realization of these systems is being achieved by structures consisting of nanotubes or fullerene molecules attached to metallic electrodes.[6,7] In Ref. 7 electron transport through superconductor-metallofullerene molecules (Gd@C_{82}) superconductor junctions was analyzed. Strong features associated with superconductivity were observed for the case of junctions containing a molecular dimer. As pointed out in Ref. 7, the observed nonmonotonic dependence of the low bias current as a function of temperature could be related to a change in the magnetic configuration of the Gd atoms. DQD systems coupled to superconducting electrodes have been theoretically analyzed in Refs. 8 and 9. However, these works considered geometries and ranges of parameters which do not correspond directly to the situation in the experiments mentioned above.

In this Brief Report we provide an analysis, based on exact diagonalizations and mean field slave boson techniques, of the interplay between the Josephson effect, Kondo correlations, and antiferromagnetic coupling in S-DQD-S systems. Like in the single S-QD-S case we identify phases in which the sign of the Josephson coupling is reversed. The situation in the S-DQD-S system is however richer from the point of view of its magnetic configuration. We show that when the system is coupled to localized spins as in the experimental situation of Ref. 7 their relative orientation can be influenced by the Josephson current through the device. We claim that these properties provide a way to control the magnetic configuration of such a nanoscale system.

The system depicted in Fig. 1 consists of two coupled quantum dots in series, placed between two superconducting electrodes. The electronic degrees of freedom are represented by a double Anderson model with a single spin-degenerate level on each QD. The corresponding Hamiltonian is given by

$$\hat{H}_{el} = \hat{H}_L + \hat{H}_R + \sum_{i,\sigma} \epsilon_{i\sigma}\hat{n}_{i\sigma} + U\sum_i \hat{n}_{i\uparrow}\hat{n}_{i\downarrow} + \hat{H}_{12} + \hat{H}_{1L} + \hat{H}_{2R},$$

$$(1)$$

where the index $i=1,2$ identify each QD; the terms $\hat{H}_L$ and $\hat{H}_R$ describe the uncoupled leads as BCS superconductors characterized by a complex order parameter $\Delta e^{i\phi_{L,R}}$. $\hat{H}_{12}$ is the coupling term between the dots given by $\hat{H}_{12} = \sum_\sigma t_{12}\hat{c}^\dagger_{1\sigma}\hat{c}_{2\sigma}+\mathrm{H.c.}$ The last two terms correspond to the coupling between the dots and the electrodes, $\hat{H}_{1L(2R)} = \sum_{k\sigma} t_{L,R}\hat{c}^\dagger_{1,(2)\sigma}\hat{c}_{kL(R)\sigma}+\mathrm{H.c.}$ The Coulomb interaction within each dot is described by the U term. The coupling of the QD's with two localized magnetic moments, which in the experiments of Ref. 7 are provided by the Gd impurities, can be modeled by an additional term in the Hamiltonian of the form

$$\hat{H}_{int} = J\vec{S}_1 \cdot \vec{\sigma}_1 + J\vec{S}_2 \cdot \vec{\sigma}_2,$$

$$(2)$$

where $\vec{\sigma}_{1,2}$ are the electronic spin operators in the dots, while $\vec{S}_{1,2}$ denote the localized spins. We assume, in accordance to Refs. 7 and 10, that the magnetic coupling, J, is much weaker than the other energies involved in the problem, which allows to introduce its effect as a perturbation in a second stage. There exists some controversy concerning the sign of J in Gd@C82 although recent studies suggest that this coupling is antiferromagnetic.[10] The actual sign of J is, however, not essential for the main effects discussed below. These studies also suggest a large magnetic moment associated to the Gd impurities, which allows to consider $\vec{S}_{1,2}$ in our model as classical. We will focus in the case of strong coupling between the QD's by taking $t_{12}/\Delta=10$, which roughly corresponds to the estimates[11] for the experimental situation of Ref. 7. The results of this reference also suggest good coupling to the leads (i.e., $t_{L,R}>\Delta$).

Insight into this problem can be provided by analyzing the $\hat{H}_{el}$ ground state properties as a function of the model param-
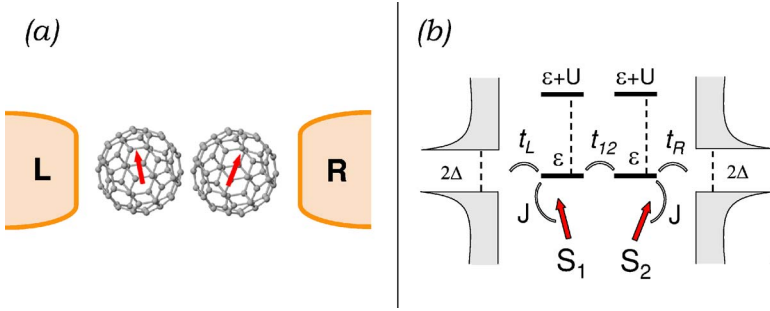
FIG. 1. (Color online) Schematic view of the studied structure (a) and involved energies (b). This system should model two fullerenes doped with Gd atoms in contact with two superconducting reservoirs (L,R).

eters. For this purpose we rely on an approximation consisting in taking the zero bandwidth limit (ZBWL) for the superconducting electrodes. The validity of this approach has been discussed for other superconducting junctions in Refs. 5 and 14. In this limit the Hilbert space of the S-DQD-S system is restricted to 4^4 states and $\hat{H}_{el}$ can be diagonalized exactly. In the superconducting case we distinguish four different ground states: the pure 0 and π states for which the energy as a function of the superconducting phase difference $\phi=\phi_L-\phi_R$ has a minimum at $\phi=0$ and π, respectively; and two intermediate phases, which are designed as $0'$ and π' depending of the relative stability of each minima.[5] Figure 2 illustrates the (ϵ,U) phase diagram for two different values of $t_R=t_L$: 2Δ [Fig. 2(a)] and 2.5Δ [Fig. 2(b)]. We show only the range of ϵ which corresponds to a charge per dot varying between 0 and 1, where the transition to the π state can take place.[12] As shown in Fig. 2, for $t_L=t_R=2\Delta$ all phases 0, $0'$, π', and π appear at the transition region. A more detailed understanding of the ground state properties is provided by analyzing nonlocal spin correlation functions of the form $\langle\vec{\sigma}_\mu\vec{\sigma}_\nu\rangle$. We choose the line in the phase diagram which corresponds to a large intradot Coulomb interaction, $U=800\Delta$, and show the evolution of these correlation functions with ϵ in Fig. 2(c) together with the occupation numbers $n_{\uparrow,\downarrow}$ for each dot. The appearance of a $1/2$ magnetic moment for the full S-DQD-S system is signaled by the broken symmetry $n_\downarrow\neq n_\uparrow$. The function $\langle\vec{\sigma}_1\vec{\sigma}_2\rangle$ measures the correlation between the electron spins in the two dots. As can be seen in

the middle panel of Fig. 2(c) it evolves continuously from 0 to $-3/4$, the latter value corresponding to a complete antiferromagnetic (AF) correlation. It is worth noticing that this AF tendency is more pronounced in the superconducting case as the presence of the superconducting gap reduces the number of low energy excitations capable to screen the spin in the dot region, i.e., it leads to a partial suppression of the Kondo correlations. In the present range of parameters, with a strong interdot hopping, the Kondo regime corresponds to the formation of a spin singlet between an electron in the bonding state of the DQD "molecule" and the electrons in the leads. This correlation is reflected in the behavior of $\langle\vec{\sigma}_{L(R)}\vec{\sigma}_{1(2)}\rangle$, which becomes increasingly negative in the Kondo regime. As can be observed in the lower panel of Fig. 2(c), Kondo correlations are strongly suppressed by superconductivity compared to the normal case. In fact, it is in the range of parameters corresponding to the Kondo region in the normal state where the π state appears. The normal state itself exhibits a transition from the Kondo to the AF regime for $-\epsilon \gg t_{12}$, signaled by $\langle\vec{\sigma}_{L(R)}\vec{\sigma}_{1(2)}\rangle\to 0$ and $\langle\vec{\sigma}_1\vec{\sigma}_2\rangle\to -3/4$. This transition roughly corresponds to the situation where the AF coupling between the dots $\sim t_{12}^2/U$ becomes larger than the AF coupling of the dots with the leads $\sim 2t_{L,R}^2/|\epsilon-t_{12}|$. If the hopping to the leads is increased, the suppression of the Kondo effect by superconductivity becomes less effective. As shown in Fig. 2(b), for $t_L=t_R=2.5\Delta$ the system exhibits only three phases (0, $0'$, and π') within the range of parameters considered. Further increase of $t_{L,R}$ would lead to a complete suppression of the π' and $0'$ phases.
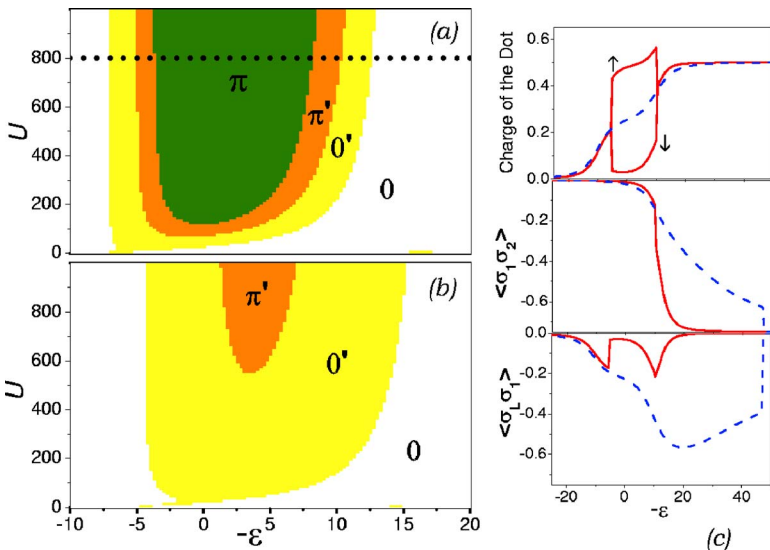

FIG. 2. (Color online) (U,ϵ) phase diagram for $t_{12}=10\Delta$, (a) $t_L=t_R=2\Delta$ and (b) $t_L=t_R=2.5\Delta$ indicating the 0, $0'$, π' and π regions. In (c) we show the ϵ dependence along the line $U=800\Delta$ indicated in (a) of (from top to bottom) the occupation number for spin up and spin down electrons, the interdot spin correlation function, and between the DQD spin and the electrodes. The dashed (solid) lines corresponds to the normal (superconducting) state.

In order to go beyond the ZBWL approximation and include the finite bandwidth of the electrodes we use an appropriate slave-boson representation of Hamiltonian equation (1). In Ref. 13 the $U \to \infty$ mean field slave-boson approach[15] was used to study the single QD system with superconducting electrodes. However, in order to describe the main features of these systems, including the possibility of unscreened magnetic moments, it is necessary to use the more general representation of Ref. 16, which is valid for finite values of U and allows for possible magnetic solutions.[17] Following Ref. 16 the auxiliary Bose fields are designed by $\hat{e}_i$ (empty state), $\hat{p}_{i\alpha}$ (single occupied state corresponding to spin σ), and $\hat{d}_i$ (double occupied state), and we define the operator $\hat{z}_{i\sigma} = (1 - \hat{d}_i^2 - \hat{p}_{i\sigma}^2)^{-1/2} (\hat{e}_i \hat{p}_{i\sigma} + \hat{p}_{i\bar{\sigma}} \hat{d}_i)(1 - \hat{e}_i^2 - \hat{p}_{i\bar{\sigma}}^2)^{-1/2}$, where $i = 1, 2$ denotes the two different QDs. In the enlarged space the Hamiltonian (1) has the form

$$\hat{H}_{el} = \hat{H}_L + \hat{H}_R + \sum_{i\sigma} \epsilon_i \hat{f}_{i\sigma}^\dagger \hat{f}_{i\sigma} + \sum_i U \hat{d}_i^\dagger \hat{d}_i$$

$$+ \sum_\sigma t_{12} (\hat{z}_{1\sigma}^\dagger \hat{z}_{2\sigma} \hat{f}_{1\sigma}^\dagger \hat{f}_{2\sigma} + \text{H.c.}$$

$$+ \sum_{k,\sigma} t_{L(R)} (\hat{z}_{1(2)\sigma}^\dagger \hat{f}_{1(2)\sigma}^\dagger \hat{c}_{kL(R)\sigma} + \text{H.c.})$$

$$- \sum_i \alpha_i \left(\hat{e}_i^\dagger \hat{e}_i + \hat{d}^\dagger \hat{d}_i + \sum_\sigma \hat{p}_{i\sigma}^\dagger \hat{p}_{i\sigma} - 1 \right)$$

$$- \sum_{i\sigma} \beta_{i\sigma} (\hat{f}_{i\sigma}^\dagger \hat{f}_{i\sigma} - \hat{p}_{i\sigma}^\dagger \hat{p}_{i\sigma} - \hat{d}^\dagger \hat{d}_i), \qquad (3)$$

where the $\hat{f}_{i\sigma}$ are fermionic operators and α_i, $\beta_{i\sigma}$ are the Lagrange multipliers corresponding to the constraints $\hat{e}_i^\dagger \hat{e}_i + \hat{d}^\dagger \hat{d}_i + \Sigma_\sigma \hat{p}_{i\sigma}^\dagger \hat{p}_{i\sigma} = 1$ and $\hat{f}_{i\sigma}^\dagger \hat{f}_{i\sigma} = \hat{p}_{i\sigma}^\dagger \hat{p}_{i\sigma} + \hat{d}^\dagger \hat{d}_i$. The particular definition of the $\hat{z}_{i\sigma}$ operators warrants that the exact solution in the $U \to 0$ limit is recovered.[16] Within a mean field approximation we replace the Bose operators in Eq. (3) by their mean values e_i, d_i, $p_{i\sigma}$, and $z_{i\sigma}$. In this approximation the Hamiltonian parameters are renormalized according to $\tilde{\epsilon}_{\sigma i} = \epsilon_i - \beta_{i\sigma}$, $\tilde{t}_{12\sigma} = t_{12} z_{1\sigma} z_{2\sigma}$, and $\tilde{t}_{L(R)\sigma} = t_{L(R)} z_{1(2)\sigma}$. The mean values of the Bose operators must be determined self-consistently by minimizing the effective action.[16]

Both the current through the dots $I = ie/\hbar \Sigma_\sigma \tilde{t}_{12\sigma} [\langle \hat{f}_{1\sigma}^\dagger \hat{f}_{2\sigma} \rangle - \langle \hat{f}_{2\sigma}^\dagger \hat{f}_{1\sigma} \rangle]$ and their occupations $n_{i\sigma} = \langle \hat{f}_{i\sigma}^\dagger \hat{f}_{i\sigma} \rangle$ can be calculated using standard Green function techniques.[18] We have solved numerically the mean field equations and computed the Josephson current through the DQD system for a certain set of parameters. In Fig. 3 we show the current-phase relation for $U = 800\Delta$, $t_{12} = 10\Delta$, and two different values of the parameter $\Gamma_{L,R} = \pi t_{L,R}^2 \rho_{L,R}(E_F)$, where $\rho_{L,R}(E_F)$ is the electrodes normal density of states at the Fermi energy. We see that for $\Gamma_L = \Gamma_R = 2.25\Delta$ the system evolves from the 0 to the π state as ϵ varies between $\sim -5\Delta$ and $\sim -2\Delta$ going back to the 0 state for $\epsilon \sim 7\Delta$. In the case of a larger coupling, $\Gamma_{L,R} = 4\Delta$, the pure π state is never reached, in good qualitatively agreement with the results obtained within the ZBWL. It is worth noticing that the occurrence of the π state requires Δ to be larger than an energy scale $\sim \sqrt{\Gamma U/2} \exp(-\pi|\epsilon - t_{12}|/2\Gamma)$, associated with the Kondo effect of the singly
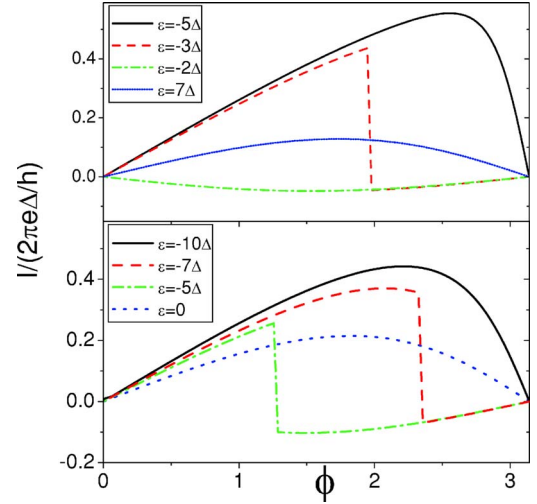

FIG. 3. (Color online) The current-phase relation for $t_{12} = 10\Delta$, $U = 800\Delta$, $\Gamma_L = \Gamma_R = 2.25\Delta$ (upper panel) and $\Gamma_L = \Gamma_R = 4\Delta$ (lower panel).

occupied bonding level, which for $t_{12}/\Gamma > 1$ can be much smaller than the effective Kondo temperature estimated for the normal DQD system.[19]

Let us now analyze how the behavior of the electronic system could influence the configuration of the localized spins by means of their magnetic coupling given by Eq. (2). One would expect that the appearance the magnetic π state could give rise to a change in this configuration with respect to the case of normal electrodes. In fact, for small J the total energy can be expanded as

$$E(h_1, h_2) \simeq E(0,0) + \sum_{\mu=1,2} a_\mu h_\mu + \sum_{\mu,\nu} a_{\mu,\nu} h_\mu h_\nu; \qquad (4)$$

where $h_\mu = J S_{\mu,z}$, $S_{\mu,z}$ being the z component of the localized spin. Notice that in general, for nonmagnetic situations, only the quadratic correction appears as in the well-known Ruderman-Kittel-Kasuya-Yoshida (RKKY) interaction.[20] For the range of parameters where the π states appear this correction would be positive leading to a AF configuration of the localized spins. However, the broken symmetry, $n_\uparrow \neq n_\downarrow$, in the π state gives rise to nonvanishing linear corrections which favor the parallel (F) configuration. This is illustrated by the insets in the upper panel of Fig. 4 which show the behavior of the total energy as a function of $h = |h_1| = |h_2|$ at $\phi = 0$ and $\phi = \pi$, respectively, in the $0'$ region of the phase diagram. A simple image of this effect is that the unscreened magnetic moment appearing in the π state acts as a local magnetic field which tends to align the localized spins. The full phase dependence of the total energy for finite J in the F and the AF configurations is depicted in the upper panel of Fig. 4. As can be observed the range of stability of the π state is increased in the F configuration, which in turn has a noticeable effect in the Josephson current (lower panel of Fig. 4). Thus, our results predict that the system switches from the AF to the F configuration as the superconducting phase is swept from 0 to π. They also suggest that in the transition region the F configuration is a metastable solution which could give rise to an hysteretic behavior as a function
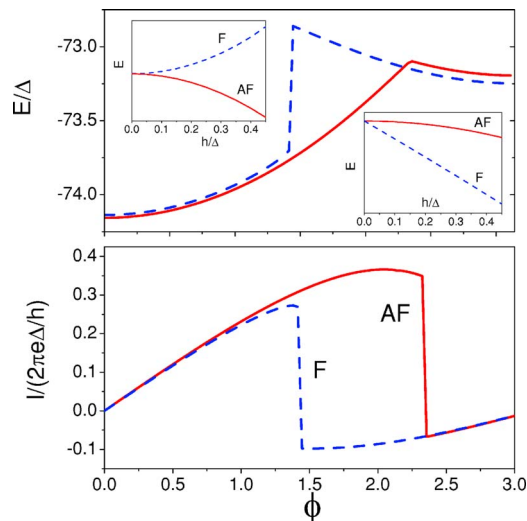
FIG. 4. (Color online) Energy (upper panel) and current-phase relation (lower panel) corresponding to the parallel (*F*, dashed line) and antiparallel (*AF*, full line) configuration of the localized spins. We have chosen $U=800\Delta$, $t_{12}=10\Delta$, $|h_1|=|h_2|=0.25\Delta$, and $\Gamma_L=\Gamma_R=2.25\Delta$. The insets show the behavior of the energy as a function of $|h_{1,2}|$ for the *F* and AF configuration at $\phi=0$ and $\phi=\pi$.

of the superconducting phase difference. Although a direct comparison with the data of Ref. 7 is not possible since the experiment was performed under nonequilibrium conditions, our results tend to support that the nonmonotonic behavior of the low bias current as a function of temperature may be indeed related to a change of the magnetic configuration of the Gd atoms. A more direct test of our predictions would require the measurement of the supercurrent in a phase biased situation.

In conclusion we have studied the magnetic and superconducting properties of a S-DQD-S system. We have shown that it can exhibit a quantum phase transition to a π state with an unscreened $1/2$ magnetic moment in the dots region. When the system is coupled to localized spins as in the experimental situation of Ref. 7 a transition from an AF to a *F* configuration can be induced by tunning the superconducting phase difference. These properties illustrate the possibility of controlling the magnetic configuration at the nanoscale by means of the Josephson effect.

Note added. Recently, we noticed the appearance of two related works.[21,22] In Ref. 21 the Josephson current through a double quantum dot was studied in the infinite *U* limit using the mean field slave-boson technique. On the other hand, Ref. 22 considers the case of a single dot coupled to a large frozen spin between superconducting leads, suggesting the possibility of controlling the $0-\pi$ transition.

[1] D. Goldhaber-Gordon, H. Shtrikman, D. Mahalu, D. Abush-Magder, U. Meirav, and M. A. Kastner, Nature (London) **391**, 156 (1998); S. M. Cronenwett, T. H. Oosterkamp, and L. P. Kouwenhoven, Science **281**, 540 (1998).

[2] R. Aguado and D. C. Langreth, Phys. Rev. Lett. **85**, 1946 (2000); H. Jeong, A. M. Chang, and M. R. Melloch, Science **293**, 2221 (2001); R. López, R. Aguado, and G. Platero, Phys. Rev. Lett. **89**, 136802 (2002); N. J. Craig, J. M. Taylor, E. A. Lester, C. A. Marcus, M. P. Hanson, and A C. Gossard, Science **304**, 565 (2004); P. S. Cornaglia and D. R. Grempel, Phys. Rev. B **71**, 075305 (2005).

[3] C. W. J. Beenaker and H. van Houten, *Single Electron Tunneling and Mesoscopic Devices* (Springer, Berlin, 1992); A. Levy Yeyati *et al.*, Phys. Rev. B **55**, R6137 (1997); G. Johansson *et al.*, *ibid.* **60**, 1382 (1999).

[4] L. Glazman and K. A. Matveev, JETP Lett. **49**, 659 (1989); A. V. Rozhkov and D. P. Arovas, Phys. Rev. Lett. **82**, 2788 (1999); F. Siano and R. Egger, *ibid.* **93**, 047002 (2004); M. S. Choi *et al.*, Phys. Rev. B **70**, 020502(R) (2004).

[5] E. Vecino, A. Martín-Rodero, and A. Levy Yeyati, Phys. Rev. B **68**, 035105 (2003).

[6] M. R. Buitelaar *et al.*, Phys. Rev. Lett. **88**, 156801 (2002); K. Gorve-Rasmussen *et al.*, cond-mat/0601371 (unpublished).

[7] A. Yu. Kasumov *et al.*, Phys. Rev. B **72**, 033414 (2005).

[8] M.-S. Choi, C. Bruder, and D. Loss, Phys. Rev. B **62**, 13569 (2000).

[9] Y. Zhu, Q. Sun, and T. Lin, Phys. Rev. B **66**, 085306 (2002).

[10] K. Furukawa, J. Phys. Chem. A **107**, 10933 (2003); C. de Nadaï *et al.*, Phys. Rev. B **69**, 184421 (2004).

[11] The estimates given in Ref. 7 are $t_{12}\sim50$ meV and $\Delta\sim0.8$ meV. One can also expect a large charging energy in these systems, i.e., $U\gg t_{12}\gg\Delta$.

[12] Recent calculations indicate that the charge occupancy in Gd-doped fullerenes corresponds to this situation, i.e., less than half-filling, see L. Senapati, J. Schrier, and K. B. Whaley, Nano Lett. **4**, 2073 (2004).

[13] Y. Avishai, A. Golub, and A. D. Zaikin, Phys. Rev. B **67**, 041301(R) (2000).

[14] I. Affleck, J.-S. Caux, and A. M. Zagoskin, Phys. Rev. B **62**, 1433 (2000).

[15] P. Coleman, Phys. Rev. B **29**, 3035 (1984).

[16] G. Kotliar and A. E. Ruckenstein, Phys. Rev. Lett. **57**, 1362 (1986).

[17] B. Dong and X. L. Lei, J. Phys.: Condens. Matter **13**, 9245 (2001); Z. Y. Zhang, *ibid.* **17**, 4637 (2005).

[18] A. Martín-Rodero, F. J. García-Vidal, and A. Levy Yeyati, Phys. Rev. Lett. **72**, 554 (1994); A. Levy Yeyati, A. Martín-Rodero, and F. J. García-Vidal, Phys. Rev. B **51**, 3743 (1995).

[19] A. Georges and Y. Meir, Phys. Rev. Lett. **82**, 3508 (1999); C. A. Büsser *et al.*, Phys. Rev. B **62**, 9907 (2000); R. Aguado and D. C. Langreth, *ibid.* **67**, 245307 (2003).

[20] G. Usaj, P. Lustemberg, and C. A. Balseiro, Phys. Rev. Lett. **94**, 036803 (2005).

[21] R. Lopez, M-S Choi, and R. Aguado, cond-mat/0603652 (unpublished).

[22] C. Benjamin, T. Jonckheere, A. Zazunov, and T. Martin, cond-mat/0605338 (unpublished).